# FINITE ELEMENT ANALYSIS OF AN ELECTROMAGNETIC ACTUATOR

**L. C. M. Oliveira**
Dept. of Computational Mechanics - FEM - UNICAMP - Av. Mendeleiev, S/N - 13083-970 - Campinas - SP - Brazil
marangoni@fem.unicamp.br

**L. O. S. Ferreira**
Dept. of Computational Mechanics - FEM - UNICAMP - Av. Mendeleiev, S/N - 13083-970 - Campinas - SP - Brazil
lotavio@fem.unicamp.br

***Abstract.*** *The prediction of the generated torque by magnetic actuators is an electromagnetic problem that involves non-linear materials and complex device geometries. This work presents a finite element model suitable for the magnetic actuator used in mm-sized induction actuated scanners. In order to validate the model a magnetic field map experiment was carried out and an overview of the spatial magnetic field distribution values was achieved. The comparison between the results have demonstrated good agreement between low-frequency measurements and the FEA model. The high frequency model and the DC model should be improved in order to adequately predicts the fields in the interest region.*

***Keywords:*** *Microscanners, FEA, Magnetic actuators, Lorentz Force, Edge-based method*

## 1. INTRODUCTION

Magnetic actuators are a viable alternative to others kinds of driving mechanisms used in mm-size Microelectro-mechanical devices, MEMS, due its capacity of handling many times more recoverable energy than other alternatives[Judy, 2001]. Its actuation principle lies in the Lorentz force due the interaction between circulating currents and electromagnetic fields[Holzer et al., 1995].

Mathematical models of magnetic actuators are based in the solution of the Maxwell equations[Lorrain et al., 1988]. Nevertheless, the obtention of analytic solutions is valid only for simple devices, being impracticable for practical problems that involves complex geometries, large air gaps and non-linear materials.

Several methods were developed to solve practical problems in electromagnetism. Nowadays, most of CAD/CAE/CAM packages are based in the finite element method in which the solution region is subdivided into a finite number of sub domains, called elements, and a trial function is postulated over each of the elements. The values of the unknown variable at each node of sub-domains is the objective of the analysis.[Cook, 1981, Bathe, 1982, Zienkiewicz, 1977].

The subject of study in this work is the electromagnetic induction mechanism, similar to that used in induction motors[Hamdi, 1998]. Its function is to generate a driving torque to move the mm-sized induction actuated scanner[Oliveira and Ferreira, 2003]. The prediction of the driving torque in such devices is a problem that involves an electromagnetic domain with large air gaps, and non-linear materials. This makes the finite element method mandatory to obtain reliable predictions for its behavior.

In this paper a finite element model for the electromagnetic induction mechanism is presented. A DC and AC analyzes were performed to understand the device behavior. By this model the electromagnetic actuation mechanism was modeled and the driving torque was predicted. The simulation results were compared with experimental and a good agreement between them was achieved.

## 2. INDUCTION ACTUATION MECHANISM

The adopted induction actuation mechanism is similar to the conventional induction motors. There are two windings: a primary, excited by an alternating current source (the stator), and a secondary, short-circuited (the armature). In this design the primary winding is housed on the stator while the plate of the scanner carries the secondary winding, as shown in Fig.1. The stator geometry is based in the magnetic bridge proposed by Brosens[Brosens, 1976]. A couple of permanent magnets are responsible for producing the DC magnetic field.

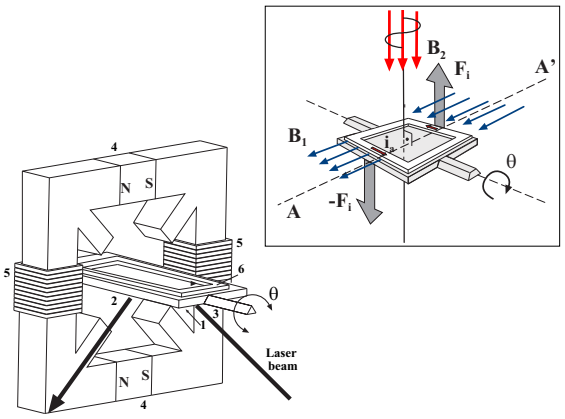


Figure 1. Induction actuated scanner (left) and the induction mechanism (top right). (1) Mirror, (2) Rotor, (3) Torsion bar, (4) Permanent magnets, (5) Driving coils, (6) Armature. A variant magnetic field, $B_2$, perpendicular to the plate, crosses the scanner armature, inducing a current $i_a$. A couple of permanent magnets generates a magnetic field, $B_1$, parallel to the plate, that interacts with the induced current producing a binary of forces, the Lorentz forces, $\pm F_i$.

Figure 1 presents a detailed sketch of the induction mechanism. A variant magnetic field, $B_2$, perpendicular to the plate, crosses the scannert's armature and induces a current $i_a$. A couple of permanent magnets generates a magnetic field, $B_1$, parallel to the plate, that interacts with the induced current producing a binary of Lorentz forces, $\pm F_i$. The induced torque rotates the plate along its axes. The strength of the torque is proportional to the induced current, DC magnetic field and geometric parameters of the device.

## 3. ELECTROMAGNETIC FINITE ELEMENT ANALYSIS

The induction actuation mechanism model was implemented using the electromagnetic module of the *ANSYS* suite that uses Maxwell's equations as the basis for magnetic field analysis[Jin, 1993]. The primary unknowns (degrees of freedom) that the finite element solution calculates are either magnetic potentials or flux. Other magnetic field quantities are derived from these degrees of freedom. Depending on the element type and element option you choose, the degrees of freedom may be scalar magnetic potentials, vector magnetic potentials, or edge flux.

In this work a 3D edge-based method[Cingoski, 1996, Webb, 1993] was used to predict the magnetic field density generated by the permanent magnets and driving coils. Two types of analyzes were performed: magnetostatic, to predict the magnetic field density due the NdFeB permanent magnets, and harmonic, to predict the magnetic field density and induced voltage in the scanner armature due variating current in the driving coils.

### 3.1 Geometry and Mesh Construction

The element adopted in the model was the SOLID117 that is a 20-node brick shape. Its the degree of freedom is the integral of the tangential component of the vector potential $A$ along the element edge.

The actual device is shown in Fig.2(a) and the model geometry in Fig.2(b). The model take advantage of the actuator symmetry, so, only one quarter of the device needed to be simulated. This approach enables a more rational use of the computational resources and a significantly decrease in the simulation times.

Due the presence of the ferromagnetic core, almost all flux-lines can be assumed inside the iron core, so, only a small distance from the stator needed to be fulfilled with air elements. The region near the armature coil, the interest region, was finely meshed, as well as, the armature.

The skin depth of the magnetic flux was calculated to use as guide to establish the mesh density through the iron core and, specially in the armature. The skin depth was calculated as follows.

$$\sigma = \sqrt{\frac{2}{\omega \mu \sigma}} \tag{1}$$

Where $\sigma$ is the skin depth, $\omega$ is the frequency in radians/second, $\mu$ and $\sigma$ are the copper permeability, Henrys/meter, and conductivity,1/Ohm-meter, respectively. The skin depth for the working frequencies of this model were, 8 mm for 80 Hz and 0.6 mm for 1 KHz. In this model was assured at least two elements through the skin depth in order to improve its reliability.

The nonlinear B-H curves for the Silicon-steel core is shown in Fig.3. The permanent magnets were supposed to be linear and the adopted properties are in Tab.1.

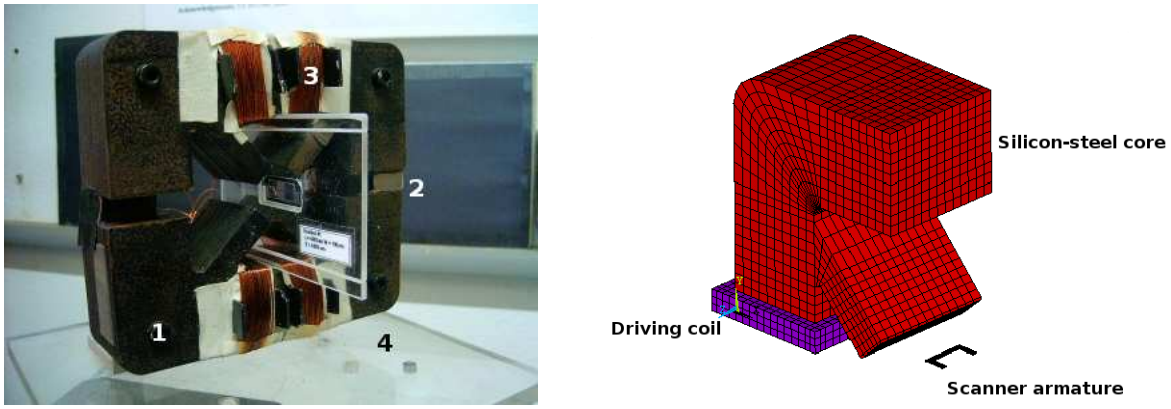


(a) (b)

Figure 2. (a) Electromagnetic actuator, 1-Silicon-steel core, 2-NdFeB magnets, 3-Driving coils, 4-Scanner, (b) FEA model of device actuator - One-quarter symmetry

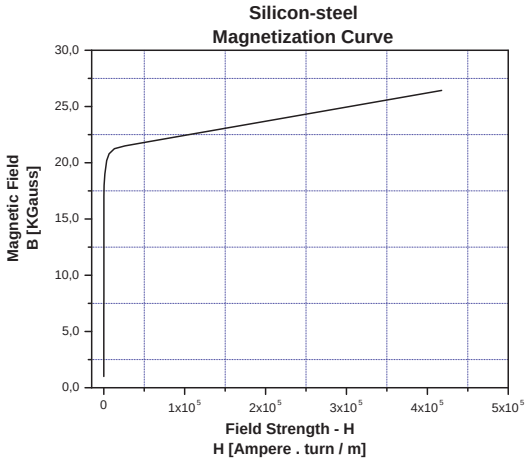


Figure 3. Silicon-Steel B-H curve

Table 1. NdFeB permanent magnet properties adopted in the model(1)

| Residual induction - Br [T] | Coercitive force - Hc [A m] | Permeability - $\mu_r$ |
|---|---|---|
| 1.14 | $8.3 \cdot 10^5$ | 1.093 |

(1) www.dextermag.com

## 4. MAGNETIC FIELD MAPPING EXPERIMENT

In order to obtain experimental values for the AC and DC magnetic field densities generated by the actuator, was necessary to map the magnetic fields in the armature device area. To do this, we have used an electromagnetic transducer(Globalmag TMAG-01T-B) in the setup presented in fig.4. Its Hall probe was attached to a micrometer and a measurement of the magnetic field along the DC and AC flux lines was carried out. A dedicated software was developed to control the instrumentation in the experiment. After a serie of 10 measurements per position, a mean was calculated, retrieved and plotted by the software. This procedure give us the profile of the magnetic fields generated by the actuator.

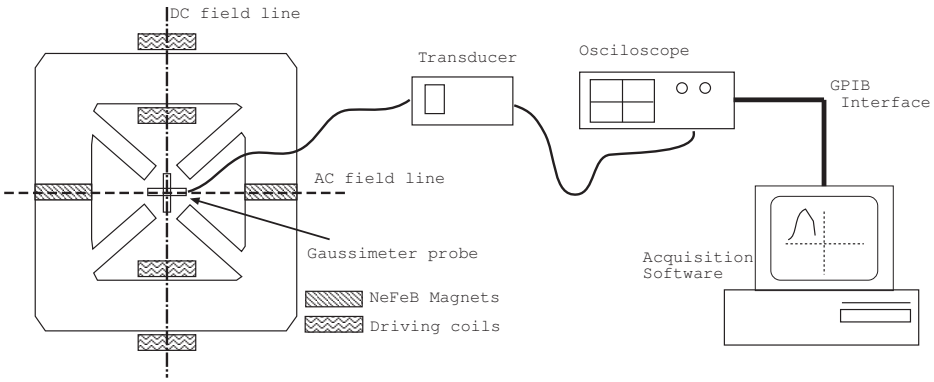


Figure 4. Magnetic field mapping experiment. A Hall probe gets the magnetic flux density at the actuator lines, AC and DC flux lines, and an oscilloscope reads the results. A dedicated acquisition software controls the instrumentation

## 5. RESULTS

The most important results from FEA simulations and measurements are shown in Fig.5 to Fig.7. The plots in Fig.5, Fig.6 and Fig.7(a) presents a map of the magnetic fields in the scanner armature region. As can be seen, there is a couple of peaks, both, in AC and DC magnetic map that represents regions with a high concentration of flux lines, in the actual stator geometry, the arms of the magnetic bridge. The region between the peaks is the region where the armature coil of the scanner must be placed, or the interest region. The DC and AC magnetic fields must be as regular as possible in this region to avoid an unbalanced generated torque. Figure 7(b) presents a profile of the FEA predicted torque as function of the driving current frequency.

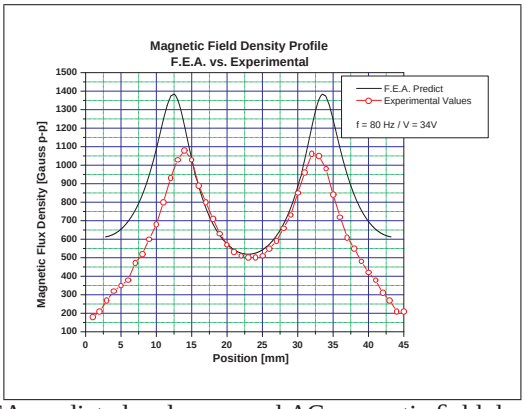


Figure 5. FEA predicted and measured AC magnetic field density at 80Hz.

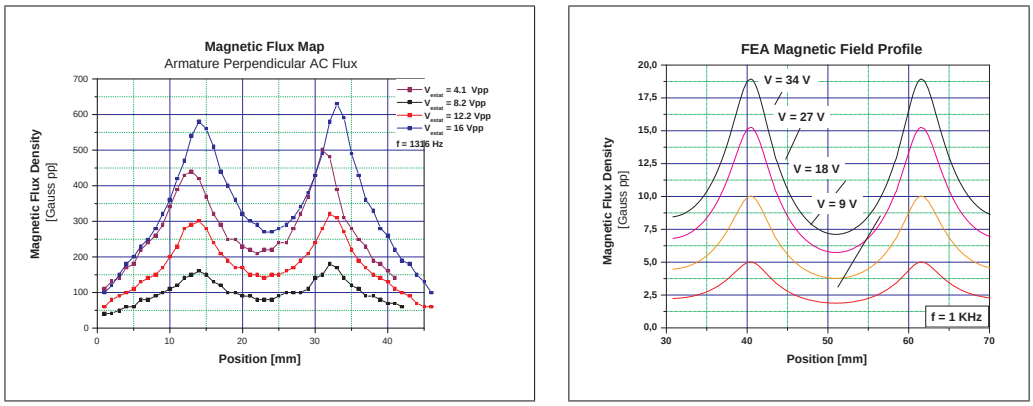


(a) (b)

Figure 6. FEA predicted and measured AC magnetic field density at 1KHz and 1.3KHz to different driving voltages. (a) Measured AC magnetic field (across the AC flux line) - 1316Hz, (b) FEA Predicted AC magnetic Field - 1KHz

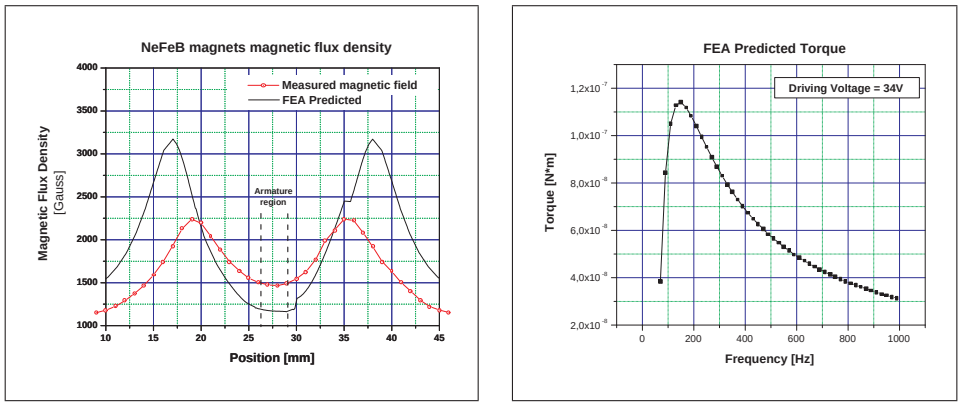


(a) (b)

Figure 7. (a) DC magnetic field comparison, (b) Induced torque as function of frequency in the armature

## 6. DISCUSSION

In this section the more relevant results obtained from electromagnetic finite element analysis and the experimental results are discussed in order to validate the results.

Figure 5 presents a comparison between the FEA predicted and measured AC and DC magnetic fields generated by the stator at 80 Hz. As can be noted there is an excellent agreement between the measured and FEA predicted values of the AC magnetic field in the interest region between the peaks. Outside of this region, there is a difference between these values. This can be due the differences in the real and modeled geometries in the region of high concentration of magnetic field lines. Refining the mesh in this region is a possible solution for this incompatibly in the results.

The measured and FEA predict results at 1KHz, fig.6(a) and fig.6(b), presents different values for the electromagnetic fields. This fact suggests that the developed FEA model are not suitable for high frequency analysis. A possible solution is the use of FEA methods based in the MVP (Magnetic Vectorial Potential), with density current (JS) instead of voltage (VLTG) loads in the model. In this way the model should be simplified due the elimination of the direct driving current dependence with the coil impedance.

The comparison between the measured and predicted magnetic flux density due the permanent magnets, Fig.7(a) shows a significant difference between the results in the interest region of the device. This can be credited to differences in the material characteristics for NdFeB magnets. A measurement of the magnetic properties of the permanent magnets used in this actuator must solve this problem.

The FEA predicted torque is shown in fig.7(b). As can be seen, the induced torque decreases with the frequency, evidencing the high inductive characteristic of the actuator. Direct measurements of this quantity, in order to validate this result, is difficult due the geometry of the device. Indirect measurements based on the deflection angle of the device are an alternative to get this.

## 7. CONCLUSIONS

In this work a finite element model for the magnetic actuator was presented and a magnetic field mapping experiment was performed to validade the model. This experiment give us an overview about the spatial distribution and values for the AC and DC magnetic field flux generated by the actuator. An interest region for placement of the device can be established, as well as, the values for the magnetic fields in it. A good agreement was achieved between the low-frequency measurements and the FEA model. The high frequency model and the DC model should be improved in order to predict adequately the fields in the interest region. The use of the MVP approach in the high frequency problem is a possible solution. Mesh improvements and a better set for the properties of the permanent magnets should improve the agreement between the DC model and the measured magnetic fields.

## 8. ACKNOWLEDGMENTS

This work was partially supported by FAPESP under project $00/10487-4$ and CNPq (MCT), process number $14040-5/2002$. The authors are grateful to CCS/UNICAMP for microfabrication facilities. Thanks to the undergraduate students Carolina and Márcio Rubbo for their help in the development of the acquisition system software.

## 9. RESPONSIBILITY NOTICE

The authors are the only responsible for the printed material included in this paper.

Bathe, K. J. ,1982, “Finite Element Procedures in Engineering Analysis”. Prentice-Hall.

Brosens, P. ,1976, “Scanning accuracy of hte moving-iron galvanometer scanner.”, Optical Engineering, Vol. 15 No. 2 pp. 95–98.

Cingoski, V. ,1996, “Study on Improved Three-Dimensional Electromagnetic Field Computations Utilizing Vector Edge Finite Elements”, PhD thesis, Hiroshima University.

Cook, R. D. ,1981, “Concepts and Applications of Finite Element Analysis”. John Wiley and Sons, New York.

Hamdi, E. S. ,1998, “Design of Small Electrical Machines”. Wiley and Sons Ltd., Baffins Lane, Chichester, England, $1_{st}$ edition.

Holzer, R., Shimoyama, I., and Miura, H. ,1995, “Lorentz force actuation of flexible thin-film aluminum.”, In “Proceedings of the IEEE/RSJ International Conference onIntelligent Robots and Systems 95”, volume 2, pages 156–161.

Jin, J. ,1993, “The Finite Element Method in Electromagnetics”. John Wiley and Sons, Inc.

Judy, J. W. ,2001, “Microelectromechanical systems (mems): fabrication, design and applications.”, Smart Materials and Structures Smart Materials and Structures, No. 10 pp. 1115–1134.

Lorrain, P., Corson, D. R., and Lorrain, F. ,1988, “Electromagnetic Fields and Waves”. W. M. Freeman and Company, 3rd edition, 580.141L893e3 (IFGW).

Oliveira, L. C. M. and Ferreira, L. O. S. ,2003, “Silicon Micromachined Double-Rotor Scanner.”, In “Proceedings of the IV Optomechatronics Conference”, volume 21, pages 634–642.

Webb, J. B. ,1993, “Edge elements and what they can do for you.”, IEEE Transactions on Magnetics, Vol. 30 No. 2 pp. 1460–1465.

Zienkiewicz, O. C. ,1977, “The Finite Element Method”. McGraw-Hill Company, London.